PCP
PLANT & CELL PHYSIOLOGY

Regular Paper

An Activity-Staining Method on Filtration Paper Enables High-Throughput Screening of Temperature-Sensitive and Inactive Mutations of Rice α-Amylase for Improvement of Rice Grain Quality

Hiromoto Yamakawa*, Rieko Hirai-Kimura, Yuriko Nakata, Masaru Nakata, Masaharu Kuroda and Takeshi Yamaguchi

Crop Development Division, Central Region Agricultural Research Center, National Agriculture and Food Research Organization (NARO), Inada 1-2-1, Joetsu Niigata, 943-0193, Japan
*Corresponding author: E-mail, hy741220@affrc.go.jp; Fax, +81-25-526-3245.
(Received December 15, 2016; Accepted February 14, 2017)

α-Amylase is a starch-hydrolyzing enzyme (EC 3.2.1.1) indispensable for germination of cereal seeds, but it is also expressed during the ripening stage. Previous studies demonstrated that the enzyme is activated in developing rice seeds under extremely hot weather and triggers a loss of grain quality by hindering the accumulation of storage starch in the endosperm. Since inactive or, preferably, heat-labile α-amylases are preferable for breeding premium rice, we developed a method for rapid screening of inactive and temperature-sensitive mutants of the enzyme by combining the random mutagenesis by error-prone PCR and an on-filter activity test of the recombinant enzyme expressed by *Escherichia coli*. This technique was applied to a major α-amylase in the developing seed, Amy3D, and the activity of the isolated mutant enzymes was verified with both the bacteria-expressed recombinant proteins and the extract from the endosperm overexpressing each of them. Then, we identified several substitutions leading to loss of the activity of amino acid residues (Leu28, Asp112, Cys149, Trp201, Asp204, Gly295, Leu300 and Cys342), as well as a variety of heat-sensitive substitutions of Asp83, Asp187 and Glu252. Furthermore, variations of the heat-labile enzymes were created by combining these heat-sensitive mutations. The effects of the respective mutations and their relationship to the structure of the enzyme molecule are discussed.

Keywords: Activity staining • α-Amylase • Grain quality • Random mutation • Rice (*Oryza sativa*) • Temperature-sensitive.

Abbreviations: DAF, days after flowering; GST, glutathione S-transferase; IPTG, isopropyl-β-D-thiogalactopyranoside; TS, temperature-sensitive; VC, vector control.

Introduction

Recent global warming is endangering the yield and quality of grain crop products. Rice plants cultivated in Asian countries often encounter high temperatures above 35°C during their ripening season. Such high temperatures impair grain filling, leading to the production of immature and chalky-appearing grains (Tashiro and Wardlaw 1991, Morita et al. 2004). Since chalky grains are fragile and prone to crack during the milling process, they are graded as low-quality grains, creating a major problem for rice-producing farmers. In contrast to the translucent endosperm of healthy grains, which consist of tightly filled polygonal starch granules, the endosperm of the chalky grains contains numerous air spaces among loosely packed round starch granules, thus reflecting the light (Zakaria et al. 2002, Tsutsui et al. 2013). Therefore, grain chalkiness is thought to be attributed to a shortage of starch filling in the mature endosperm. Previous multi-omic studies revealed that high temperatures abolished starch accumulation by a combination of a reduction in starch biosynthesis and induction of starch degradation in the developing grains (Lin et al. 2005, Yamakawa et al. 2007, Yamakawa and Hakata 2010), and the prevention of starch degradation by suppressing the expression of genes for a single starch-hydrolyzing enzyme, α-amylase (EC 3.2.1.1), was sufficient to reduce chalky grains when the developing grains were exposed to high temperatures (Hakata et al. 2012), thus proposing a new strategy to develop high temperature-tolerant rice plants.

Loss-of-function genetic mutation offers an alternative to abolish α-amylase in the developing grains. In the rice genome, eight genes encoding α-amylase, namely *Amy1A*, *Amy1C*, *Amy2A*, *Amy3A*, *Amy3B*, *Amy3C*, *Amy3D* and *Amy3E*, were found. According to the RiceXPro database (http://ricexpro.dna.affrc.go.jp/), *Amy3A* and *Amy3D* are expressed in the endosperm of developing seeds while *Amy3E* is expressed in the embryo of the seeds, and *Amy1A*, *Amy1C*, *Amy3A*, *Amy3D* and *Amy3E* were up-regulated by high temperature (Hakata et al. 2012). On the other hand, a proteome study identified Amy1A, Amy3B, Amy3C, Amy3D and Amy3E as expressed isoforms in germinating seeds (Nanjo et al. 2004). All of these isoforms have conserved residues that are indispensable for activity: the catalytic triads, as well as two histidines required for transition state stabilization, and a tryptophan at the starch-binding site, corresponding to Asp180, Glu205, Asp291, His93, His290 and Trp279 of barley Amy1

Plant Cell Physiol. 58(4): 658–667 (2017) doi:10.1093/pcp/pcx030, Advance Access publication on 21 February 2017, available online at www.pcp.oxfordjournals.org

(Søgaard et al. 1993, MacGregor et al. 2001). Substitution of these residues by other amino acids abolished the glycolytic activity. However, the significance of amino acids other than the above residues awaits a comprehensive analysis.

α-Amylase is activated immediately after seed imbibition and is indispensable for the hydrolysis of stored starch to nourish the embryo and establish the growth of young seedlings. Complete deletion of the activity may inhibit seed germination. For conventional cultivation, rice seeds germinate at moderate temperatures less than 28°C following adequate water imbibition at low temperatures such as 10°C. On the other hand, the temperature at which α-amylase is activated and abolishes grain quality at the ripening stage is around 35°C. Therefore, in considering the development of premium grain quality rice plants, the heat-sensitive mutation of α-amylase genes is preferable.

In this study, we developed an applied method to identify inactive or heat-sensitive mutants of α-amylase by employing error-prone PCR mutagenesis and screening of the recombinant α-amylase expression library by activity staining. By applying this method to the rice *Amy3D* gene, whose expression was induced by high temperatures in the developing seeds (Hakata et al. 2012), novel loss-of-activity and a variety of heat-sensitive mutations were identified. The activity and heat stability of those mutant enzymes and their in vivo activity in the developing seeds were investigated.

Results

Characteristics of rice α-amylase isoforms

Prior to the screening of inactive and heat-sensitive α-amylase, the properties of innate α-amylase isoforms encoded by the rice genome were investigated. Eight isoforms, designated Amy1A (IRGSP accession No. Os02g0765600), Amy1C (Os02g0765300), Amy2A (Os06g0713800), Amy3A (Os09g0457400), Amy3B (Os09g0457600), Amy3C (Os09g0457800), Amy3D (Os08g0473900) and Amy3E (Os08g0473600), were found to have the amino acids consisting of catalytic triads, two aspartate and one glutamate, conserved. Considering the overall identity and similarity among their peptide sequences after removal of putative N-terminal signal peptides (O'Neill et al. 1990, Ochiai et al. 2014), the pairs of Amy1A and Amy1C and of Amy3B and Amy3C are very closely homologous isoforms to each other (Supplementary Fig. S1A). First, the enzyme properties were analyzed with the recombinant α-amylases individually produced by *Escherichia coli* by two different methods: a colorimetric activity assay using an oligosaccharide substrate and the activity staining of gels containing the glucan-chained carbohydrate, starch. As summarized in Supplementary Fig. S1E, Amy1C and Amy3D exhibited high activities against both the oligosaccharide and the glucan chains (Supplementary Fig. S1B, C). Amy2A, Amy3B and Amy3C showed relatively low activities against the oligosaccharide and weak but varied extents of activities in the starch gel assay, while the activity of Amy3A was very weak or below the detection limit in the conditions used. Interestingly, Amy3E exhibited moderate activity against the oligosaccharide, but it showed very weak activity on the starch gel, whereas Amy1A gave strong bands on the glucan-containing gels, but it showed weak activity in the oligosaccharide assay. These isoforms varied in terms of thermostability. Amy3D retained most of its activity after incubation at 40°C for 10 min, but was almost inactivated by heat treatment at 50°C (Supplementary Fig. S1D). Amy3B and Amy3C were unstable since they lost activity at 40°C, while Amy1A was stable enough to retain 15% activity after incubation at 50°C. Next, the properties of individual isoforms were investigated with extracts from the developing endosperms that overexpress each α-amylase. Under these experimental conditions, the vector control (VC) extract gave trace levels of activity. Consistent with the above case of recombinant proteins, the extract of the Amy3D expresser exhibited strong activity against both the oligosaccharide and starch (Supplementary Fig. S2A, B). In this experiment, the Amy3C extract was similar to that of Amy3D, although it gave another extra band on the starch gel. Amy1A and Amy1C gave strong bands in the starch gels, but the activity against the oligosaccharide was relatively weak. In contrast, the Amy3E extract showed moderate activity with the oligosaccharide, but no activity was detected against starch. Thus, Amy1A apparently prefers long-chain glucans as its substrates, whereas Amy3E prefers oligosaccharides. Again, a variety of levels of thermotolerance were observed with the endosperm extracts, although they endured much higher temperatures than the corresponding recombinant isoforms (Supplementary Fig. S2C, D). The Amy1A and Amy1C extracts were robust enough to retain most of their activity up to 80°C, while Amy2A and Amy3A lost their activity completely at 70°C.

During the above experiments with the recombinant and endosperm-overexpressed α-amylases, Amy3D exhibited strong activity and intermediate thermostability. Conveniently, a large amount of Amy3D was expressed as a soluble protein in *E. coli*, whereas only a small fraction was obtained in a soluble form for the other isoforms. Moreover, the pilot examination demonstrated that the Amy3D-expressing bacterial colonies exhibited intense starch-lytic activities and gave distinguishable halos in the following activity screening assay, but those expressing the other α-amylases did not. Therefore, the screening was performed using the Amy3D expression vector.

Screening of inactive Amy3D mutants

To generate random mutations on Amy3D, we took advantage of error-prone PCR by adding Mn^{2+} to the PCR mixture (**Fig. 1A**). The error rate was optimized by varying the Mn^{2+} concentration. As shown in Supplementary Fig. S3, the number of nucleotide substitutions per Amy3D cDNA rose by increasing the concentrations of $MnSO_4$ and $MnCl_2$. Along with this, the substitution of 2.5, 12.5, 2.5 and 10.0 amino acid residues occurred per mature Amy3D peptide when Mn^{2+} was supplied with 0.15 mM $MnSO_4$, 0.50 mM $MnSO_4$, 0.15 mM $MnCl_2$ and 0.50 mM $MnCl_2$, respectively. Furthermore, the application of Mn^{2+} in a high concentration, as much as 0.5 mM, resulted in nucleotide deletions with high frequencies (one in four sequenced clones in both the $MnSO_4$ and $MnCl_2$ additions). Among the types of nucleotide substitution, transitions such as A to G, T to C, G to A and C to T were most frequent compared

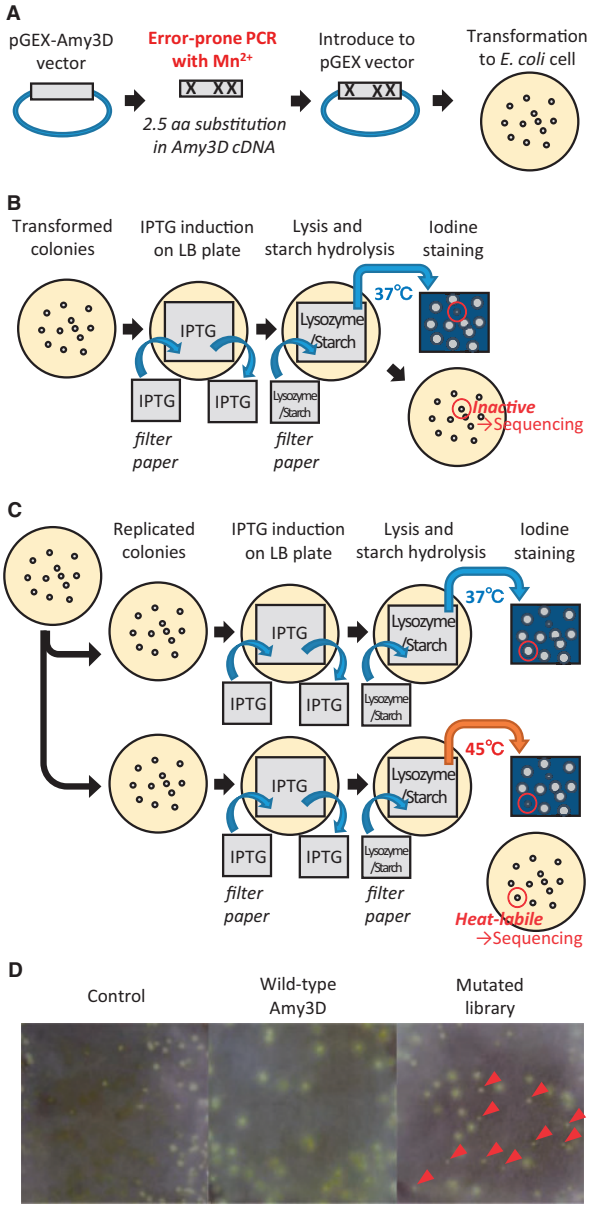

Fig. 1 Schematic representation of the procedure for screening α-amylase mutants. (A) Random mutagenesis of the *Amy3D* coding sequence. The expression vector harboring *Amy3D*, which was mutated by error-prone PCR, was introduced into *E. coli*. (B) Screening for inactive *Amy3D*. A variety of mutated Amy3D proteins were induced on the LB plates and analyzed for enzyme activity with starch-imbibed filter paper. (C) Screening for temperature-sensitive *Amy3D*. A pair of replicated plates were subjected to the activity screening at 37 and 45°C, and the sizes of halos were compared. (D) Representative images of activity detection. Iodine-stained filters for the control vector, the wild-type Amy3D expression vector and the mutated Amy3D library, which have been reacted at 37°C, are shown. Inactive clones are indicated with red arrowheads. The bacterial colonies and halos occasionally appeared yellowish, since bacterial debris hampers staining of starch by iodine.

with transversions in these conditions. Considering the above mutation frequency, 0.15 mM $MnSO_4$ and 0.15 mM $MnCl_2$ were suitable in terms of screening efficiency and were selected for the following experiments.

The method for screening inactive Amy3D mutants consisted of the following four steps: (i) the transformation of the *E. coli* host cells with approximately 2,400 colony-forming units (cfu) of the bulked pGEX vectors (10 plates each of $MnSO_4$- and $MnCl_2$-mutated bulks with the concentration of 120 cfu per plate), each of which contained the independently created different mutations; (ii) the induction of mutated Amy3D expression by contacting the bacterial colonies with isopropyl-β-D-thiogalactopyranoside (IPTG)-imbibed filter paper; (iii) lysis of the bacteria and starch hydrolysis by overlaying another filter paper containing the lysozyme and starch; and (iv) the detection of the α-amylase activity as halos by staining with iodine solution (**Fig. 1B**). By picking the colonies which did not develop halos (indicated with red arrowheads in **Fig. 1D**), 199 candidate clones of inactive mutants were selected. The DNA sequencing of their Amy3D-coding regions revealed that a large portion of the clones contained multiple nucleotide substitutions. By extracting the clones with a single amino acid residue substituted, 24 cases of substitution were chosen for the mutations possibly causing the loss of enzyme activity. To verify the effect of those substitutions on α-amylase activity, 24 types of mutation were created on the pGEX-Amy3D vector one by one and then subjected to the activity test. As shown in Supplementary Fig S4, all the candidate mutations, except for K222E (which means the Lys222 was substituted with glutamate, hereinafter) and W299R, gave no or reduced sizes of halos.

The loss of activity may be caused by either the unstabilization or inactivation of the mutated Amy3D. To distinguish the above cases, the *E. coli* cells expressing the mutant forms of Amy3D were lysed, and then the crude proteins were separated into soluble and insoluble fractions and analyzed by SDS–PAGE. As shown in **Fig. 2A**, a substantial portion of the mutant proteins, namely C149Y, D204G, K222E, V279A and W299R, were distributed into the soluble fraction, as unmutated native Amy3D was, while the other variants were mostly fractionated into the insoluble matter, suggesting that the mutants other than the above five lost their activity by the unstabilization of the enzyme molecules. Then, the soluble mutants were purified and subjected to a colorimetric activity assay. Among the five mutants, C149Y and D204G lost their activities completely, whereas the activities of K222E, V279A and W299R were similar to that of the unmutated wild-type Amy3D (**Fig. 2B**), indicating that C149Y and D204G remained soluble but lost activity.

Screening of temperature-sensitive Amy3D mutants

By raising the temperature up to 45°C during the above step (iv), in which α-amylase hydrolyzed the starch, the thermostability of the mutated enzymes was verified (**Fig. 1C**). Choosing the clones which exhibited small or no halos on the filter incubated at 45°C but large halos on the 37°C plot, as shown in Supplementary Fig. S5, from 1,400 colonies transformed with the bulked vectors (14 plates each of $MnSO_4$- and $MnCl_2$-mutated bulks with the concentration of 50 cfu per plate), allowed identification of 34 candidates for the

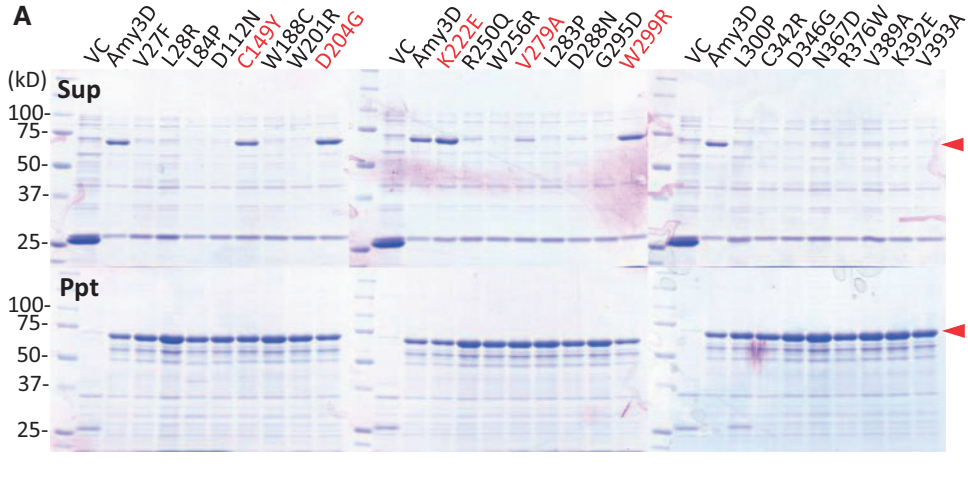

Fig. 2 Halo-negative mutants of Amy3D. (A) Solubility of the mutant proteins analyzed by SDS–PAGE. The soluble (Sup) and insoluble (Ppt) proteins extracted from *E. coli* expressing mutant Amy3D–GST fusion proteins (corresponding to 10 μl of culture) were separated by SDS–PAGE and visualized by Coomassie Brilliant Blue (CBB) staining. Arrowheads indicate the recombinant Amy3D proteins (fused to the GST tag). Soluble mutants are indicated by red characters. (B) α-Amylase activity of the soluble Amy3D mutants. The recombinant Amy3D proteins were purified following excision of the GST tag and subjected to α-amylase activity assay.

heat-labile Amy3D mutants. The candidate clones were cultured in the liquid medium, induced by application of IPTG and subjected to purification of the mutant proteins. Then, the 23 independent mutants were obtained as soluble proteins, whereas the rest of the clones expressed a large portion of the enzyme in the insoluble fraction. The activity analysis with the soluble purified enzymes following pre-incubation at varying temperatures revealed that nine mutants, designated TS01, TS03, TS07, TS08, TS10, TS11, TS20, TS21 and TS22, were temperature-sensitive (TS) and lost activity at lower temperatures than the unmutated Amy3D (Supplementary Fig. S6C). In the absence of the heat treatment, TS01, TS03, TS08 and TS10 exhibited high activities, and TS21 showed a moderate activity, whereas the activities of TS07, TS11, TS20 and TS22 were relatively low (Supplementary Fig. S6A). As the temperature of the heat incubation increased, TS07, TS08 and TS11 lost half of their activities below 43°C, and the other TS mutants did so at 45–47°C, while the wild-type Amy3D retained half of its activity over 48°C (Supplementary Fig. S6E). Among those TS mutants, TS08 was unique, since it showed a similar or even higher level of activity compared with the wild-type Amy3D, but it was extremely sensitive to the elevated temperatures and lost a large part of its activity below 45°C.

In order to identify the amino acid substitution that is crucial for the decreased thermostability of the enzyme, the Amy3D coding regions of the above nine TS mutants were sequenced. The alignment of the peptide sequences deduced from the nucleotide sequences of the TS mutants proposed 14 cases of amino acid substitution as the possible mutations lowering the heat stability (Supplementary Fig. S7), although the involvement of the C-terminal extension, YAAAS, of TS11 in heat instability could not be excluded. It is noteworthy that most of the substituted amino acid residues, except for F307L, are not located in either of the catalytic domains.

To verify the effect of the 14 identified substitutions on the thermostability of Amy3D, the pGEX-Amy3D vector harboring each of the mutations was generated by site-directed mutagenesis one by one, and the mutated enzymes were expressed by the bacteria, purified and subjected to the activity test. The degree of thermosensitivity of the resulting single residue-substituted variants was in agreement with that of the corresponding TS mutants identified by the screening. Again, D83G, the solitary mutation found in TS08, gave a similar level of activity to the unmutated Amy3D without the heat treatment, but lost the majority of the activity below 45°C (Supplementary Fig. S6B, J). Similarly, A277T, F307L, Y236C and C119R exhibited patterns of thermostability close to that of the corresponding TS mutants, TS10, TS11, TS21 and TS22, respectively (Supplementary Fig. S6K, L, N, O). However, E252G was somewhat more sensitive to the moderately high temperature of 45°C than the corresponding mutant, TS03, in the repeated experiments, even though both have the same single substitution (Supplementary Fig. S6H). Among the substitution mutants for TS01, I363T was inactivated at a lower temperature than K123M, indicating that the decreased heat stability of TS01 is attributed to I363T rather than K123M (Supplementary Fig. S6G). On the other hand, both C130N and N245S, corresponding to the substitutions in TS20, had lowered thermostability, while the decrease in activity prior to the heat treatment may be due to the former substitution (Supplementary Fig. S6M). The decrease in the extent and thermostability of TS07 would be attributed mostly to V260I and both D187V and V260I, respectively (Supplementary Fig. S6I). Taken together, D83G, D187V, E252G and F307L had a high impact on lowering the inactivation temperature, although C119R, C130G, Y236C, N245S, V260I, A277T, I363T and K418R had weak effects. The extent of activity was decreased greatly by C119R and F307L and moderately by C130G, Y236C and V260I. The substitutions D83G, D187V and E252G are

unique, since they lowered the thermostability without affecting the activity prior to the heat treatment.

In order to create more heat-labile α-amylases, mutants harboring multiple thermosensitive substitutions were produced by combining D83G, D187V and E252G. As shown in **Fig. 3**, the double substitution D187V/E252G lowered thermostability. The temperature for losing half of the activity was 43.0°C, which was below that of the single mutations D187V (47.0°C) and E252G (46.4°C) (**Fig. 3D**). Similarly, D83G/D187V and D83G/E252G lowered the half-inactivating temperature to <25.0 and 29.1°C, respectively, from the 30.8°C of the D83G single substitution, although their intact activities prior to heat incubation decreased to some extent. However, the triple substitution D83G/D187V/E252G abolished a large portion of activity even prior to the heat treatment (**Fig. 3A**). Thus, combinations such as D83G/D187V and D187V/E252G achieved additive enhancement of thermosensitivity without a large decrease of innate activity.

Characterization of inactive and temperature-sensitive Amy3D mutants in developing seeds

The in planta properties of Amy3D mutant forms isolated by the screenings were verified by comparing the activity of the extracts from the developing endosperm that overproduced individual mutants with that of the endosperm overexpressing wild-type Amy3D. Since overexpression of active α-amylases often produces chalky grains by de novo starch degradation in the developing endosperm (Asatsuma et al. 2006), the appearance of mature grains in the transgenic rice was observed as a hallmark of the starch-lytic activity. The overexpression of wild-type Amy3D resulted in 10- to 100-fold stronger activities in the endosperm compared with the VC, which is consistent with Supplementary Fig. S2, and produced severe chalkiness on the grains of the first generation following transformation with a segregation ratio of 3 : 1 (chalky to translucent) (**Fig. 4**). The mutants C149Y and D204G, whose recombinant proteins lost activity completely (**Fig. 2**), exhibited background levels of activity similar to the VC transgenic endosperm and yielded translucent grains, while K222E, V279A and W299R gave levels as high as 10- to 100-fold of the control and produced chalky grains, as the wild-type Amy3D did. The mutants, whose recombinant proteins were insoluble, were divided into two categories: those showing high activities with chalky grains, V27F, L84P, W188C, R250Q, W256R, L283P, D288N, D346G, N367D, R376W, V389A, K392E and V393A, and those presenting background activities with translucent grains, L28R, D112N, W201R, G295D, L300P and C342R. Thus, L28R, D112N, C149Y, W201R, D204G, G295D, L300P and C342R were the substitutions abolishing activity when expressed in the developing endosperm.

The thermostability of the temperature-sensitive D83G mutant was examined using the extract from developing endosperm overproducing the mutant form. Although it still retained a majority of the activity at 60°C, a 6°C decrease of the inactivating temperature was achieved by the single substitution when it was compared with the intact Amy3D (**Fig. 5**).

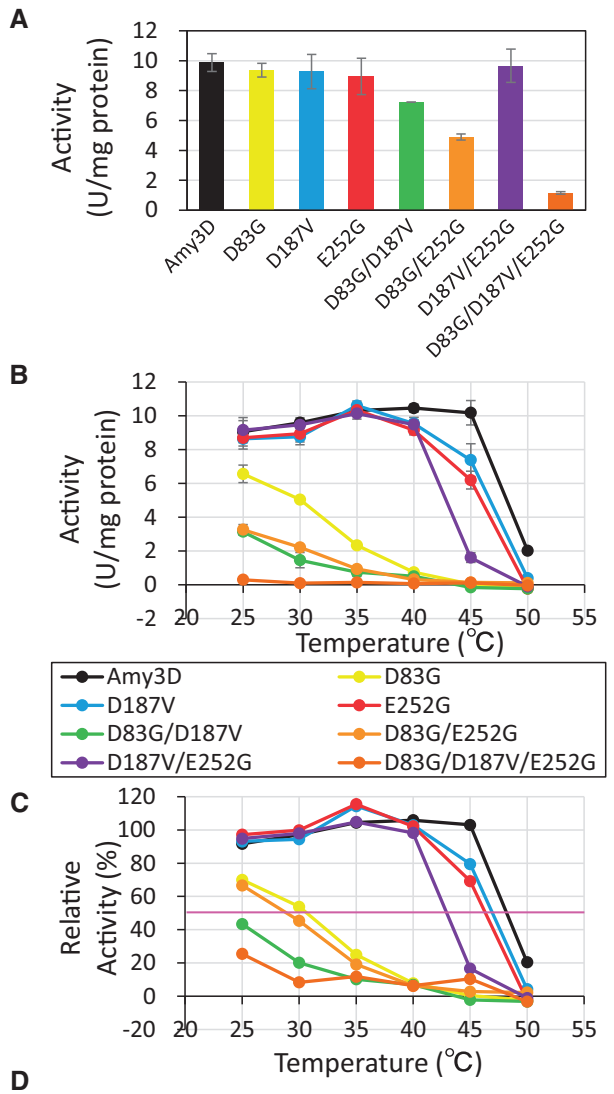

D

	Half-inactivating temperature (°C)
Amy3D	48.3
D83G	30.8
D187V	47.0
E252G	46.4
D83G/D187V	< 25.0
D83G/E252G	29.1
D187V/E252G	43.0
D83G/D187V/E252G	< 25.0

Fig. 3 Effect of accumulation of temperature-sensitive (TS) mutations on thermostability of Amy3D. (A) Activity of Amy3D mutants prior to the heat treatment. (B) Activity of the mutants following incubation at the indicated temperatures for 10 min. (C) Relative activities of the mutants. The activities of the respective mutants prior to the heat treatment were set to 100%. (D) Half-inactivating temperature for the respective mutants.

Discussion

In contrast to the broad industrial demands for high temperature-tolerant α-amylase, high temperature-sensitive α-amylase

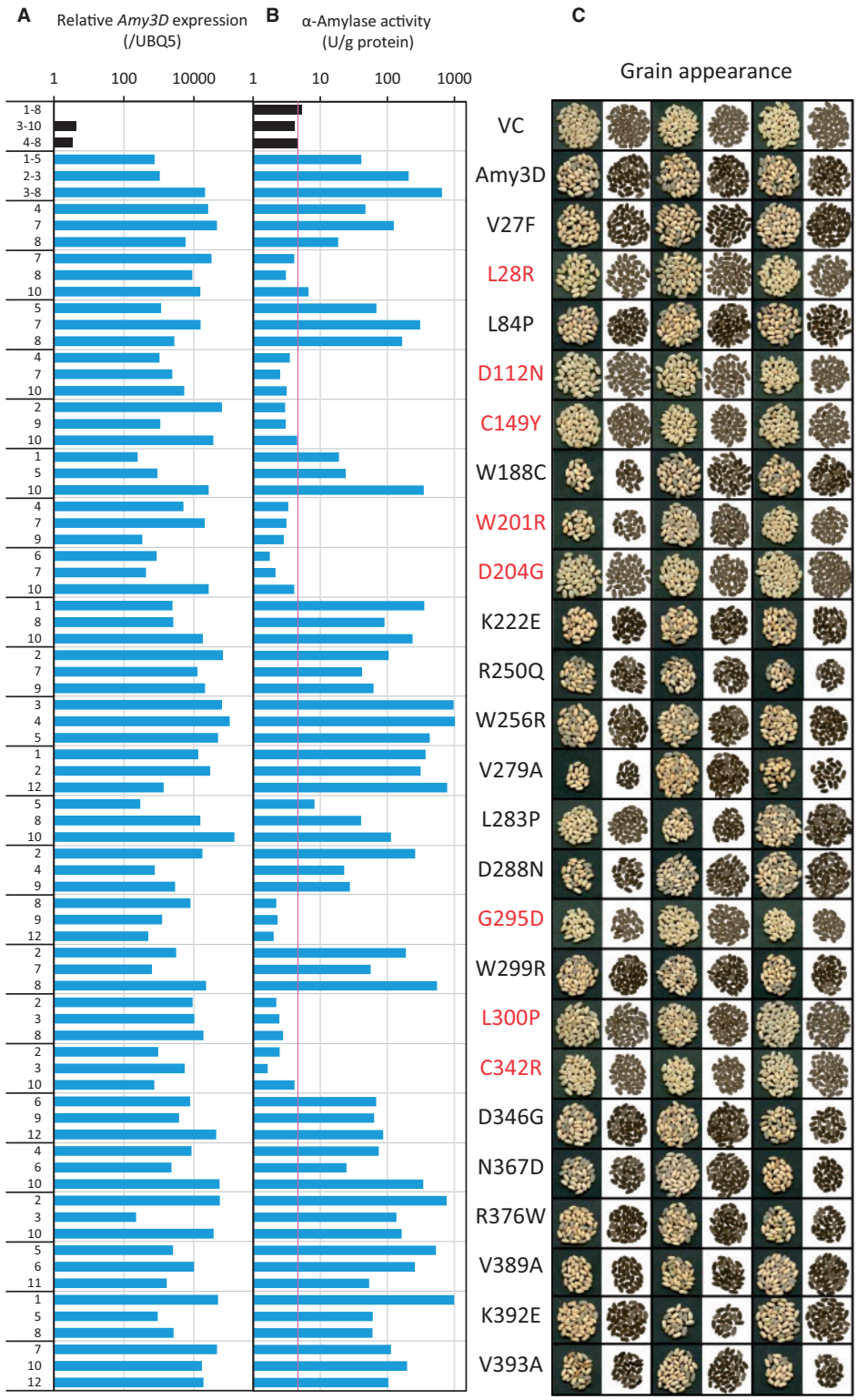

Fig. 4 α-Amylase activity during mid-ripening stage and grain appearance at maturity of the transgenic rice seeds overexpressing Amy3D with various substitutions. (A) The amount of the *Amy3D* transcript relative to that of *UBQ5* was determined by quantitative RT-PCR. (B) α-Amylase activity was determined for the extracts from developing grains at 15 d after anthesis. (C) Grain images, corresponding to three respective lines, were captured with both reflected and transmitted light. The mutants presenting background activities with translucent grains are indicated by red characters.

A

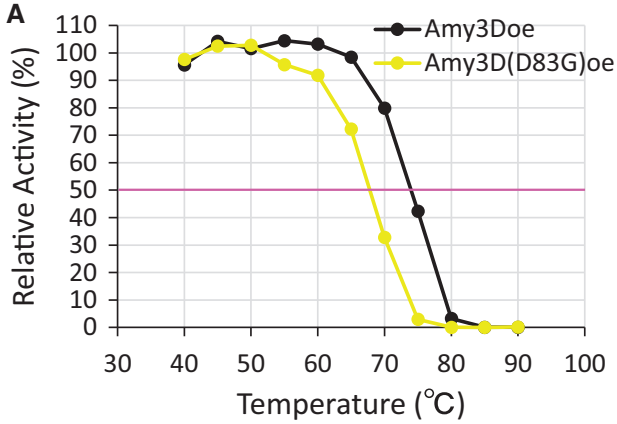

B

	Half-inactivating temperature (°C)
Amy3D	73.9
D83G	67.8

Fig. 5 Thermostability of α-amylase mutants overexpressed in rice endosperm. (A) Activity of the Amy3D and the D83G mutant following incubation at the indicated temperatures for 10 min. The activities of the respective mutants prior to the heat treatment (257.3 and 404.0 U g^{-1} protein, respectively) were set to 100%. (B) Half-inactivating temperature for the respective forms.

has not been explored well. The previous finding that α-amylase induced by high temperatures in the ripening seeds deleteriously affects the quality of the cereal products (Hakata et al. 2012) prompted us to explore heat-sensitive varieties of the enzyme. Although α-amylase is indispensable for remobilization of the storage starch during seed germination, this process is conducted at relatively low temperature below 28°C in the conventional culture of rice seedling. In contrast, ripening rice plants often encounter high temperatures around 35°C in the paddy field, which activate the starch-lytic enzyme, leading to the loss of grain quality. Therefore, creating α-amylases which are inactivated at such high temperatures offers a preferable tool for the breeding of premium rice.

The established screening method employing the recombinant protein expression system of *E. coli* allowed the rapid identification of as many as 199 inactive candidate clones in approximately a week. It shortened the duration by 6 months and omitted the need for vast cultivation spaces, which are normally required for the generation and screening of a large number of transgenic rice plants. The subsequent one-by-one evaluation of the selected mutants with a single amino acid residue substituted using the recombinant proteins, as well as the transgenic endosperm extracts overexpressing the corresponding forms, identified eight novel inactive substitutions, two of which (C149Y and D204G) yielded soluble recombinant proteins and six of which (L28R, D112N, W201R, G295D, L300P and C342R) were insoluble (**Figs. 2**, **4**). Sorted by the solubility of the recombinant proteins, the ratios of the number of the mutants confirmed inactive in the rice endosperm to that of the candidates identified beforehand by the recombinant protein analysis were 100% (two of two clones) and 31.6% (six of 19 clones) for soluble inactive and insoluble proteins, respectively. Such high true-positive ratios of 'inactive in the rice endosperm' to 'inactive or unstable in the bacteria' proves that the bacterial expression screening method is sufficiently rapid and efficient.

The screening for TS mutants with the bacterial expression library identified a variety of substitutions lowering the inactivation temperature, such as D83G, D187V and E252G (**Fig. 3**; Supplementary Fig. S6). However, the half-inactivating temperature of the most heat-labile D83G in its overexpressing endosperm extract (67.8°C) was much higher than that of the corresponding recombinant protein (30.8°C), although the substitution lowered thermostability in both preparations (**Figs. 3**, **5**). Therefore, more heat-sensitive mutations are required to counteract the unusual starch hydrolysis by the enzyme in the ripening grain at high temperatures around 35°C. Since the combination of multiple mutations further decreased the thermotolerance of the recombinant forms (**Fig. 3**), accumulation of more temperature-sensitive substitutions in the molecule may yield more heat-labile enzymes. Considering thermostability of the native α-amylase isoforms, the recombinant proteins prepared by the induced expression in *E. coli* are relatively heat labile and lost half of their activity at moderate temperatures such as <30°C (Amy3B and Amy3C), 38°C (Amy1C and Amy3E), 43°C (Amy2A) and 45°C (Amy1A and Amy3D) (Supplementary Fig. S1). In contrast, the extracts from developing rice seeds overexpressing the respective isoforms retained half of the activity until higher temperatures around 53°C (Amy3A), 63°C (Amy2A), 74°C (Amy3B, Amy3C, Amy3D and Amy3E) and 82°C (Amy1A and Amy1C) (Supplementary Fig. S2), although the optimum reaction temperatures for Amy3D and Amy3E, purified from rice suspension cultured cells, are much lower at 37 and 26°C, respectively (Mitsui et al. 1996). This discrepancy of the thermostability may be attributed to modifications of the enzyme such as glycosylation. Rice Amy1A possesses an *N*-linked glycosylation consensus site, ^{265}NAT^{267} (Ochiai et al. 2014), and the native form of Amy1A is glycosylated (Terashima et al. 1994). Since removal of the sugar chain decreased its activity (Terashima et al. 1994), glycosylation is required for the stabilization of the enzyme under heat stress conditions in the case of Amy1A. However, this consensus is conserved for Amy1C, but not for the other isoforms. Therefore, glycosylation at other sites or unknown post-translational modification may confer thermostability in Amy2A, Amy3B, Amy3C, Amy3D and Amy3E.

The inactive and temperature-sensitive substitutions of amino acid residues identified in this study were dispersed throughout the enzyme molecules, as shown in blue and orange, respectively, in Supplementary Fig. S7. When their locations were compared with those of the known conserved catalytic domains (Søgaard et al. 1993, MacGregor et al. 2001), Asp112, Trp201 and Asp204 were located in the first, second and second conserved catalytic domains, respectively, while Leu300 resided at the surface-binding site, thus confirming that these residues are indispensable for activity. However, the change of Leu28, Cys149, Gly295 and Cys342, which are located outside of the known catalytic elements, also caused

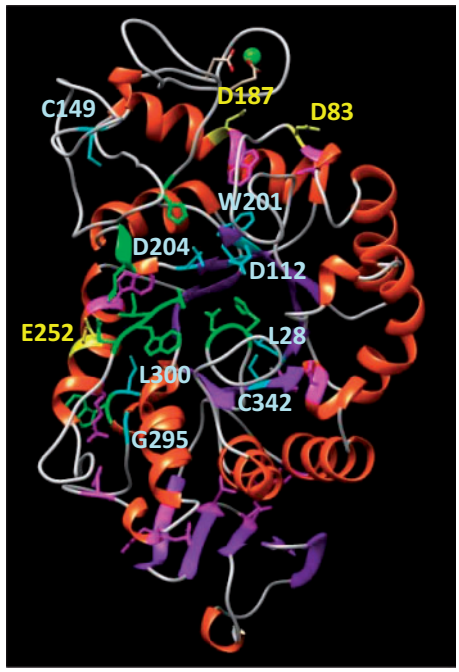

Fig. 6 Location of amino acid residues responsible for the enzyme activity in the Amy3D molecule. The structure of the Amy3D molecule was modeled on a barley α-amylase (SMTL id of 1bg9.1.A) by SWISS-MODEL, since its peptide sequence exhibited the highest identity to that of Amy3D among available templates. The conserved catalytic residues, the identified residues whose substitution abolished the activity (Leu28, Asp112, Cys149, Trp201, Asp204, Gly295, Leu300 and Cys342), thermostability-related residues (Asp83, Asp187 and Glu252) and a calcium ion are indicated in green, blue, yellow and green, respectively. The residues whose substitutions did not affect the activity in the endosperm extracts were indicated in pink.

a complete loss of activity (**Figs. 2**, **4**). Cys149, whose substitution did not affect the solubility of the recombinant protein, might be involved in the control of the redox status, although the mechanism underlying the redox regulation of the plant α-amylase activity remains unclear. Considering the spatial location of these residues in the Amy3D molecule modeled on a barley α-amylase (**Fig. 6**), the side chains of Leu28, Cys149, Trp201, Gly295 and Cys342 are oriented in the molecules. Mutations of L28R, C149Y, W201R, G295D and C342R would cause destruction of the molecular structure. In particular, mutations other than W201R replace small residues with large residues. Therefore, such structural interference would abolish the enzyme activity. For another possible explanation for the mode of inactivation, Leu28 and Cys342, as well as Asp112, Trp201 and Asp204, are located inside and orientated toward the central catalytic pocket, and all of the substitutions (L28R, D112N, W201R, D204G and C342R) are accompanied by a change in the electric charge, such as negative to neutral and neutral to positive, leading to a deficiency of electrons and the disturbance of the hydrolysis reaction. On the other hand, the residues whose substitutions retained activity in the endosperm extracts (**Fig. 4**) are in the peripheral α-helix coil and β-sheet structures, as shown in pink in **Fig. 6**. The major TS mutations (indicated in yellow in **Fig. 6**) occurred on the peripherally located amino acid residues, Asp83, Asp187 and Glu252, not at the position causing structural interference, and all were accompanied by changes from acidic to neutral amino acids. The mechanism underlying the decrease in thermostability by this charge change remains to be determined.

In conclusion, the brief screening procedure allowed a rapid and efficient identification of inactive and heat-labile mutations for α-amylase. The amino acid residues which were shown to be critical for the activity are conserved for all rice α-amylase isoforms except for Leu300. Among the heat-sensitive residues, Asp83 is preserved for all the isoforms, while Asp187 was unchanged in almost all α-amylases other than Amy1A and Amy1C, and Glu252 is also conserved with the exception of Amy2A, raising the possibility that the properties of the other isoforms may be modified in a similar manner by the same substitution. Recently, pin-point mutation of the intended nucleotides of arbitrarily selected genes is becoming feasible by genome editing tools such as CRISPR/Cas9 nucleases and its associated nucleotide exchanging methodologies (Shan et al. 2013, Mikami et al. 2015, Osakabe and Osakabe 2015). Considering the reported expression profiles of the respective isoforms, Amy1A and Amy3D, which were detected in both developing and germinating seeds should be the targets for TS modification to circumvent disturbance in germination, whereas inactive modification would be enough for Amy3A, which is not expressed during germination. The optimization of endogenous α-amylase genes by introducing the identified valuable mutations on the above conserved residues offers a novel tool for breeding rice plants with premium grain quality.

Materials and Methods

Expression and purification of recombinant α-amylases

Considering putative signal peptides deduced by previous studies (O'Neill et al. 1990, Ochiai et al. 2014), DNA fragments corresponding to the mature α-amylase peptides were generated by PCR using the full-length cDNA plasmids provided by the National Institute of Agrobiological Sciences and the primers listed in Supplementary Table S1, except for those of Amy1C and Amy3C. The fragments of Amy1C and Amy3C were amplified with cDNA derived from developing seeds at the milky stage overexpressing the respective α-amylase genes and the primers listed in Supplementary Table S1, The amplified cDNA fragments were digested with *Eco*RI–*Not*I or *Bam*HI–*Not*I, as indicated, and then cloned into the same restriction sites of the pGEX-6P-1 vector (GE Healthcare), yielding pGEX-Amy1A to pGEX-Amy3E vectors to allow expression of those α-amylases fused to a glutathione *S*-transferase (GST) at its N-terminus. *Escherichia coli* BL21 (DE3) were transformed with the resulting vectors and cultured at 30°C until the optical density at 600 nm reached 0.6. α-Amylase proteins were induced by the addition of 0.5 mM IPTG, followed by further culture at 22°C for 15 h. The cells were collected by centrifugation at 3,700 × *g* for 5 min at 4°C and lysed in PBS buffer (10 mM Na_2HPO_4, 140 mM NaCl, 2.7 mM KCl, 1.8 mM KH_2PO_4, pH 7.4) by incubation with 1 mg ml^{-1} lysozyme for 30 min, followed by sonication. After centrifugation at 20,000 × *g* for 10 min at 4°C, the soluble protein fraction was applied to a glutathione–Sepharose spin column, GST SpinTrap (GE Healthcare), and the recombinant α-amylase was eluted by digestion with PreScission Protease (GE Healthcare) in 50 mM

Tris–HCl, 150 mM NaCl and 1 mM dithiothreitol (DTT), pH 7.5, according to the manufacturer's protocol. The protein concentration was determined using a protein assay kit (Bio-Rad) with bovine serum albumin as the standard. The homogeneity of the purified recombinant α-amylase proteins was verified by SDS–PAGE on 10% polyacrylamide gels (Laemmli 1970) and staining with Coomassie Brilliant Blue R-250.

Enzyme assay of recombinant α-amylases

Activity of recombinant α-amylase was quantitatively determined using a maltopentaose-based colorimetric substrate kit (Kikkoman Biochemifa Company) according to the manufacturer's protocol. The reaction was started by mixing 9 μl of the α-amylase sample (containing 100 ng of the protein) with 45 μl of the substrate solution and 45 μl of the enzyme solution, carried out by incubation at 37°C for 60 min, and then terminated by adding 180 μl of the stop solution. The activity was determined by measuring the absorbance using a Multiskan GO microplate reader (Thermo Fisher Scientific). One unit of α-amylase activity was defined as the amount of enzyme needed to release 1 μmol CNP (2-chloro-4-nitrophenyl) from N3-G5-β-CNP per minute. To verify thermostability, an aliquot of the respective α-amylase was incubated at the indicated temperature for 10 min prior to the above assay.

Activity against starch was verified by the native PAGE/in-gel activity staining method. The recombinant α-amylase proteins were separated on non-denaturing 7.5% (w/v) polyacrylamide gels containing 0.3% (w/v) potato tuber starch (Sigma) by the methods of Davis (1964). The electrophoresis was performed at 4°C at a constant current of 15 mA. To detect the α-amylase activity, the gel was rinsed twice and then incubated at 30°C for 2 h with 50 mM sodium acetate, pH 5.3, containing 3 mM $CaCl_2$. The α-amylase activity was visualized as transparent bands by staining the gel with 0.1% I_2/1% KI solution.

Screening of inactive and heat-sensitive Amy3D mutants

The coding region for the mature Amy3D peptide in the pGEX-Amy3D expression vector was mutated randomly by error-prone PCR as follows. The DNA fragment corresponding to the mature peptide of Amy3D was amplified with 1 U of Takara LA Taq (TAKARA BIO) and 0.1 ng of the pGEX-Amy3D plasmid in a 20 μl reaction mixture containing 1 × LA PCR buffer II, 0.4 mM dNTP, 2.5 mM $MgCl_2$, various concentration of $MnSO_4$ or $MnCl_2$, and 0.5 μM of the primers listed in Supplementary Table S1. Amplification was carried out with a profile of 30 s denaturation at 98°C, followed by 30 cycles of 98°C for 15 s, 55°C for 30 s and 72°C for 2 min. The resulting 1.3 kb product was fractionated on a 1.0% agarose gel and then eluted. The mutated fragment was cloned into the pGEX vector by the *Dpn*I method. Briefly, 200 ng of the fragment was subjected to the 20 μl reaction mix, which contains 1 × Phusion HF reaction buffer, 0.2 mM dNTP, 20 ng of the pGEX-Amy3D vector and 0.1 U of Phusion HF DNA polymerase (New England Biolabs). The reaction was performed with a profile of 1 min denaturation at 98°C, followed by 25 cycles of 98°C for 30 s, 60°C for 50 s and 72°C for 7 min. Then, 15 μl of the resulting mix was digested with 10 U of *Dpn*I (New England Biolabs) and used for the transformation of *E. coli* JM109 competent cells. The transformed cells were cultured in bulk in liquid LB medium containing 50 μg ml^{-1} ampicillin, and then the plasmid consisting of a mixture of a variety of mutated pGEX-Amy3D was prepared.

For screening inactive Amy3D mutants (**Fig. 1B**), approximately 120 cfu (corresponding to 5–15 ng) of the above bulky plasmid were transformed to the BL21 (DE3) competent cells, and the cells were spread to an 8 cm LB medium Petri dish. Following an overnight culture at 37°C, the expression of the recombinant proteins was induced by further incubation at 30°C for 3 h with the plate surface covered by a filter paper that was immersed in 3 mM IPTG in advance. After removal of the filter paper, the bacterial colonies were lysed by contact with another filter paper, which was prepared by absorbing 0.1% soluble starch, drying and immersing in 1 mg ml^{-1} lysozyme immediately before usage. Following incubation at 37°C for 2 h, the filter papers were stripped, and the α-amylase activity was visualized by spraying them with the 0.1% I_2/1% KI/0.5% acetic acid solution. During the final incubation, the starch absorbed in the filter paper was hydrolyzed around the colonies, which expressed active Amy3D, thus forming large white halos when stained by the iodine solution, whereas such halos were not formed around the colonies which did not express the active form of the enzyme. The colonies on the original LB plates corresponding to the halo-negative clones were picked for LB culture, and then the harbored pGEX-Amy3D plasmid was prepared and subjected to DNA sequencing.

For screening heat-sensitive mutants (**Fig. 1C**), two replicate plates were taken from the original plates using a replica-plating tool (Bel-Art Products) and subjected to IPTG induction and subsequent detection with the starch-imbibed paper as described above, except that one plate was incubated at 37°C and the other at 45°C. The clones exhibiting a large halo at 37°C but a small or no halo at 45°C were selected, and the corresponding colonies on the original plates were subjected to plasmid preparation and DNA sequencing.

The activity and thermosensitivity of the selected inactive and heat-sensitive mutants were confirmed using single amino acid residue-substituted Amy3D proteins, which were independently generated by site-directed mutagenesis of the pGEX-Amy3D vector by the *Dpn*I method (Ishii et al. 1998).

Generation of transgenic rice plants expressing mutated Amy3D and determination of α-amylase activity

The rice 10 kDa prolamin promoter and terminator were employed for developing the endosperm-specific expression vector of Amy3D. The 10 kDa prolamin promoter was amplified from rice genomic DNA using the primer set in Supplementary Table S1. The resulting fragment had a *Hin*dIII restriction site at the 5′ end and *Xba*I plus *Bam*HI restriction sites at the 3′ end. In addition, the *Spe*I restriction site in the flanking region of the 10 kDa prolamin promoter was deleted by nucleotide substitution in the reverse primer. The pZH2B10ik binary vector (Kuroda et al. 2010) was double digested by *Hin*dIII and *Bam*HI to remove the RNAi (RNA interference) cassette (10 kDa prolamin promoter and aspartic protease intron); then, the newly amplified 10 kDa prolamin promoter was inserted instead to produce the pZH2B10dT vector. Then, the coding region of *Amy3D* was amplified by PCR using the full-length cDNA plasmids provided by the National Institute of Agrobiological Sciences and the primers listed in Supplementary Table S1. The resulting fragment was cloned into the *Xba*I and *Kpn*I restriction sites of the pZH2B10dT binary vector, yielding the pZH2B10dT-Amy3D vector used for the overexpression of Amy3D in the developing endosperm. Then, the binary vectors for overexpression of the Amy3D mutants were generated by site-directed mutagenesis of the pZH2B10dT-Amy3D vector by the *Dpn*I method.

The obtained overexpression vectors and pZH2B vector (Kuroda et al. 2010) (for the control lines) were introduced into *Agrobacterium tumefaciens* strain EHA101 by electroporation. Rice (*Oryza sativa* cv. 'Nipponbare') was transformed as described previously (Toki 1997). Six transgenic T_0 seedlings regenerated from hygromycin-resistant calli were transplanted into a plastic container filled with 700 ml of culture soil (containing 0.18 g each of nitrogen, phosphate and potassium) and grown in an air-conditioned greenhouse at 29°C/24°C under natural light. The developing caryopses at 15 days after flowering (DAF) were used for determination of transcript levels and α-amylase activity. Approximately 45 DAF, mature grains were harvested and photographed.

To confirm the overexpression of *Amy3D* genes in the transgenic plants, RNA was extracted from three developing caryopses using an RNeasy plant mini kit (Qiagen). First-strand cDNA was synthesized from each preparation of the RNA using a PrimeScript RT reagent kit (TAKARA BIO) and an oligo(dT) primer. Then, real-time quantitative PCR was performed with the Thermal Cycler Dice Real Time system TP850 (TAKARA BIO) using SYBR Premix Ex Taq (TAKARA BIO) according to the manufacturer's instructions. The PCR conditions were as follows: 95°C for 10 s, 40 cycles of 95°C for 5 s and 60°C for 30 s. The gene-specific primers used for amplification are listed in Supplementary Table S1. The *UBQ5* primer pair (Jain et al. 2006) was used as an internal standard for normalization. Relative gene expression was determined by the ΔΔCt method.

For measurement of α-amylase activity in the developing grains, three caryopses were frozen in liquid nitrogen and crushed with a Multi-beads Shocker (MB301; Yasui Kikai). The resulting powder was suspended in a 10-fold volume of extraction buffer (10 mM HEPES-KOH, pH 7.5, 1 mM $CaCl_2$) for

3 h at 4°C. Following two rounds of centrifugation at 20,000 × *g* for 5 min at 4°C, the supernatant was used to determine α-amylase activity with the above α-amylase measurement kit. The assay was performed as described above, except the reaction was terminated at 20 min. The data were corrected by the protein content of the respective extracts determined by the protein assay kit (Bio-Rad) with bovine serum albumin as the standard.

Supplementary data

Supplementary data are available at PCP online.

Funding

This work was supported by the Ministry of Agriculture, Forestry, and Fisheries of Japan [Genomics-based Technology for Agricultural Improvement, grant No. IVG3001] and the Ministry of Education, Culture, Sports, Science, and Technology of Japan [Japan Society for the Promotion of Science Grant-in-Aid for Scientific Research (C) (15K07279) to H.Y.].

Disclosures

The authors have no conflicts of interest to declare.

References

Asatsuma, S., Sawada, C., Kitajima, A., Asakura, T. and Mitsui, T. (2006) α-Amylase affects starch accumulation in rice grains. *J. Appl. Glycosci.* 53: 187–192.

Davis, B.J. (1964) Disc electrophoresis II: method and application of human serum proteins. *Ann. N.Y. Acad. Sci.* 121: 404–427.

Hakata, M., Kuroda, M., Miyashita, T., Yamaguchi, T., Kojima, M., Sakakibara, H., et al. (2012) Suppression of α-amylase genes improves quality of rice grain ripened under high temperature. *Plant Biotechnol. J.* 10: 1110–1117.

Ishii, T.M., Zerr, P., Xia, X.M., Bond, C.T., Maylie, J. and Adelman, J.P. (1998) Site-directed mutagenesis. *Methods Enzymol.* 293: 53–71.

Jain, M., Nijhawan, A., Tyagi, A.K. and Khurana, J.P. (2006) Validation of housekeeping genes as internal control for studying gene expression in rice by quantitative real-time PCR. *Biochem. Biophys. Res. Commun.* 345: 646–651.

Kuroda, M., Kimizu, M. and Mikami, C. (2010) A simple set of plasmids for the production of transgenic plants. *Biosci. Biotechnol. Biochem.* 74: 2348–2351.

Laemmli, U.K. (1970) Cleavage of structural proteins during the assembly of the head of bacteriophage T4. *Nature* 227: 680–685.

Lin, S.K., Chang, M.C., Tsai, T.G. and Lur, H.S. (2005) Proteomic analysis of the expression of proteins related to rice quality during caryopsis development and the effect of high temperature on expression. *Proteomics* 5: 2140–2156.

MacGregor, E.A., Janeček, Š. and Svensson, B. (2001) Relationship of sequence and structure to specificity in the α-amylase family of enzymes. *Biochem. Biophys. Acta* 1546: 1–20.

Mikami, M., Toki, S. and Endo, M. (2015) Comparison of CRISPR/Cas9 expression constructs for efficient targeted mutagenesis in rice. *Plant Mol. Biol.* 88: 561–572.

Mitsui, T., Yamaguchi, J. and Akazawa, T. (1996) Physicochemical and serological characterization of rice α-amylase isoforms and identification of their corresponding genes. *Plant Physiol.* 110: 1395–1404.

Morita, S., Shiratsuchi, H., Takanashi, J. and Fujita, K. (2004) Effect of high temperature on grain ripening in rice plants. Analysis of the effect of high night and high day temperatures applied to the panicle and other parts of the plant. *Jpn. J. Crop Sci.* 73: 77–83.

Nanjo, Y., Asatusma, S., Itoh, K., Hori, H. and Mitsui, T. (2004) Proteomic identification of α-amylase isoforms encoded by *RAmy3B/3C* from germinating rice seeds. *Biosci. Biotechnol. Biochem.* 68: 112–118.

Ochiai, A., Sugai, H., Harada, K., Tanaka, S., Ishiyama, Y., Ito, K., et al. (2014) Crystal structure of α-amylase from *Oryza sativa*: molecular insights into enzyme activity and thermostability. *Biosci. Biotechnol. Biochem.* 78: 989–997.

O'Neill, S.D., Kumagai, M.H., Majumdar, A., Huang, N., Sutliff, T.D. and Rodriguez, R.L. (1990) The α-amylase genes in *Oryza sativa*: characterization of cDNA clones and mRNA expression during seed germination. *Mol. Gen. Genet.* 221: 235–244.

Osakabe, Y. and Osakabe, K. (2015) Genome editing with engineered nucleases in plants. *Plant Cell Physiol.* 56: 389–400.

Shan, Q., Wang, Y., Li, J., Zhang, Y., Chen, K., Liang, Z., et al. (2013) Targeted genome modification of crop plants using a CRISPR–Cas system. *Nat. Biotechnol.* 31: 686–688.

Søgaard, M., Kadziola, A., Haser, R. and Svensson, B. (1993) Site-directed mutagenesis of histidine 93, aspartic acid 180, glutamic acid 205, histidine 290, and aspartic acid 291 at the active site and tryptophan 279 at the raw starch binding site in barley α-amylase 1. *J. Biol. Chem.* 268: 22480–22484.

Tashiro, T. and Wardlaw, I.F. (1991) The effect of high temperature on kernel dimensions and the type and occurrence of kernel damage in rice. *Aust. J. Agric. Res.* 42: 485–496.

Terashima, M., Kubo, A., Suzawa, M., Itoh, Y. and Katoh, S. (1994) The role of the N-linked carbohydrate chain of rice α-amylase in thermostability and enzyme kinetics. *Eur. J. Biochem.* 226: 249–254.

Toki, S. (1997) Rapid and efficient *Agrobacterium*-mediated transformation in rice. *Plant Mol. Biol. Rep.* 15: 16–21.

Tsutsui, K., Kaneko, K., Hanashiro, I., Nishinari, K. and Mitsui, T. (2013) Characteristics of opaque and translucent parts of high temperature stressed grains of rice. *J. Appl. Glycosci.* 60: 61–67.

Yamakawa, H. and Hakata, M. (2010) Atlas of rice grain filling-related metabolism under high temperature: joint analysis of metabolome and transcriptome demonstrated inhibition of starch accumulation and induction of amino acid accumulation. *Plant Cell Physiol.* 51: 795–809.

Yamakawa, H., Hirose, T., Kuroda, M. and Yamaguchi, T. (2007) Comprehensive expression profiling of rice grain filling-related genes under high temperature using DNA microarray. *Plant Physiol.* 144: 258–277.

Zakaria, S., Matsuda, T., Tajima, S. and Nitta, Y. (2002) Effect of high temperature at ripening stage on the reserve accumulation in seed in some rice cultivars. *Plant Prod. Sci.* 5: 160–168.